Modeling the output performances of the apodized fiber grating diode lasers by transfer matrix method

J. LI, Z.-M. WU, T. DENG, G.-Q. XIA*

School of Physics, Southwest University, Chongqing 400715, China

Based on the transfer matrix method, by which the limitations of Lang-Kobayashi model and equivalent cavity model can be partly overcome, the output characteristics of the apodized fiber grating diode lasers (FGLs) have been theoretically investigated. The results show that with the change of the maximum of the refractive index modulation depth Δn_0, both the number and the location of the modes will vary; under certain parameters, single mode operation with the side-mode suppression ratio (SMSR) more than 40dB can be achieved.

(Received July 31, 2008; accepted August 14, 2008)

Keywords: Fiber grating diode lasers, Transfer matrix method, Gaussian apodized fiber grating

1. Introduction

With the development of dense wavelength division multiplexing (DWDM) technology, the light source with narrow line-width and good wavelength stability has been required due to the channel spacing of a DWDM system. Compared with the distributed feedback (DFB) diode laser, the fiber grating diode lasers (FGLs) have some advantages such as small size, narrow linewidth, low insertion loss, high coupling efficiency and good wavelength stability, which makes FGLs excellent candidate light source of DWDM system and a research hot [1-4].

At present, most of the related theoretical investigations on FGLs mainly use two traditional models of external cavity semiconductor lasers (ECSLs). One is Lang-Kobayashi model, which considers external optical feedback as a perturbation of internal cavity field and presupposes the number of longitudinal modes and their wavelengths before any simulations are undertaken [5-6]. The other is equivalent cavity model, where the effect of front facet of laser diode (facing the external cavity) and the external cavity is combined and represented with an equivalent reflection coefficient [1,2,4,7]. However, there exist some limitations during analyzing the ECSLs on the basis of above models. So Pierce et al. [8] proposed the transfer matrix method to study the output characteristics of the multimode external cavity semiconductor laser. This method can partly overcome the limitations of above two approaches. In this paper, we extend this method to the apodized FGLs. Compared to ordinary fiber grating (FG), the apodized FG can significantly reduce the sidelobes of the reflection spectrum, and therefore has a better wavelength selectivity for FGLs [9-10]. After adopting the transfer matrix method, the output characteristics such as the optical spectrum and the side-mode suppression ratio have been simulated numerically on the basis of the multimode rate equations.

2. Theory

A FGL is composed of four sections, LD chip, air gap between the LD facet and fiber, fiber and FG. Their length is L_d, L_a, L_e, L_g, respectively. The refractive index for each section is denoted by η. The longitudinal position of the interface between each section is z_0, z_1, z_2, z_3, z_4, respectively. The structure is bounded by two regions with air on the left of z_0 and fiber on the right of z_4.

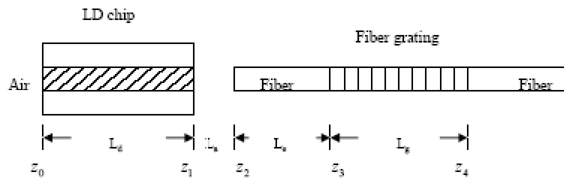

Fig. 1. Schematic of a fiber grating diode lasers.

According to the coupled-mode theory, each section is assigned a backward-propagating field amplitude A_m and a forward-propagating field amplitude B_m, such that the total field E_m in each section is given by

$$E_m = A_m e^{-ik_m z} + B_m e^{ik_m z} \tag{1}$$

where k_m is the complex propagation constant of the mth section and can be expressed as $k_m = \frac{\omega}{c}(\eta_m + i\chi_m)$, η_m is the refractive index of the mth section. As for the laser gain section, the refractive index η_1 is a variable and can be described as $\eta_1=\eta_{a1}+b(N-N_0)$, where η_{a1} is the refractive index of the gain medium corresponding to the carrier density N_0, b is the slope of the refractive index changed with N. X_m is related to the material gain g_m by the expression $X_m=-\frac{c}{\omega}\frac{g_m}{2}$. Because the LD chip is filled with the gain medium, its propagation constant is given by $k_1 = \frac{\omega}{c}\eta_1 - i\frac{g_1}{2}$. In the other sections, there is not gain and the propagation constant is $k_m = \omega\eta_m/c$. According to the Eq. (1), the equation interlinking the field amplitudes at either end of the FGL system is written with the following matrix form

$$\begin{pmatrix} A_5 \\ B_5 \end{pmatrix} = Q(z_4)Q(z_3)Q(z_2)Q(z_1)Q(z_0)\begin{pmatrix} A_0 \\ B_0 \end{pmatrix} \tag{2}$$

where the matrix $Q(z_0)$, $Q(z_1)$,$Q(z_2)$ are of the form

$$Q(z_m) = \begin{pmatrix} \frac{k_{m+1}+k_m}{2k_{m+1}} e^{i(k_{m+1}-k_m)z_m} & \frac{k_{m+1}-k_m}{2k_{m+1}} e^{i(k_{m+1}+k_m)z_m} \\ \frac{k_{m+1}-k_m}{2k_{m+1}} e^{-i(k_{m+1}+k_m)z_m} & \frac{k_{m+1}+k_m}{2k_{m+1}} e^{-i(k_{m+1}-k_m)z_m} \end{pmatrix} \tag{3}$$

The phase-shifting matrix of the fiber is

$$Q(z_3) = \begin{pmatrix} \exp(-ik_3Le) & 0 \\ 0 & \exp(ik_3Le) \end{pmatrix} \tag{4}$$

As for apodized FG, it can be divided into M sections and the length of each section is Δz. As long as M is large enough, each section can be seen as a uniform FG, the matrix of the ith section $Q_i(z_4)$ is [11-12]

$$Q_i(z_4) = \begin{pmatrix} \cosh(\gamma_B\Delta z) + i\frac{\hat{\sigma}}{\gamma_B}\sinh(\gamma_B\Delta z) & i\frac{\kappa}{\gamma_B}\sinh(\gamma_B\Delta z) \\ -i\frac{\kappa}{\gamma_B}\sinh(\gamma_B\Delta z) & \cosh(\gamma_B\Delta z) - i\frac{\hat{\sigma}}{\gamma_B}\sinh(\gamma_B\Delta z) \end{pmatrix} \tag{5}$$

where the 'ac' cross-coupling coefficient is $\kappa = \frac{\pi}{\lambda}\nu\Delta n$, $\gamma_B = \sqrt{\kappa^2 - \hat{\sigma}^2}$, the 'dc' self-coupling coefficient is $\hat{\sigma} = \delta + \sigma$, the detuning is $\delta = 2\pi n_{eff}(\frac{1}{\lambda} - \frac{1}{\lambda_B})$, the 'dc' period-averaged coupling coefficient is $\sigma = \frac{2\pi}{\lambda}\Delta n$, where Δn is the average refractive index change of FG. The Bragg wavelength of FG is $\lambda_B = 2n_{eff}\Lambda$, Λ is the period, n_{eff} is the effective refractive index of FG. The refractive index distribution of the core of uniform FG is given by

$$n(z) = n_{eff} + \Delta n\cos(2\pi z/\Lambda) \tag{6}$$

Here the refractive index distribution of the Gaussian apodized FG is described as

$$n(z) = n_{eff} + \Delta n\cos(2\pi z/\Lambda) \tag{7}$$

where $\Delta n = \Delta n_0 f(z)$,Δn_0 is the maximum of the refractive index modulation depth, $f(z)$ is Gaussian apodized function and is giver by [9-10]

$$f(z) = \exp[-G(\frac{z}{Lg})^2] \tag{8}$$

where G is the parameter of the Gaussian apodized function.

The total transfer matrix of FG is

$$Q(z_4) = Q_M(z_4)\cdot Q_{M-1}(z_4)\cdot\ldots\cdot Q_i(z_4)\cdot\ldots\cdot Q_1(z_4) \tag{9}$$

The phase shift matrix of the apodized FG is given by

$$Q'(z_4) = \begin{pmatrix} \exp(-ik_4Lg) & 0 \\ 0 & \exp(ik_4Lg) \end{pmatrix} \tag{10}$$

According to the Eq. (2), since there should be no incoming electromagnetic fields, the amplitudes A_5 and B_0 are set to zero. Under this condition, Eq. (2) can then be solved numerically for the complex propagation constant of the gain section k_1. Therefore, the wavelength and threshold gain of each possible laser mode can be obtained.

The steady-state multimode rate equations of laser diode (LD) are given by [13]

$$0 = \frac{dN}{dt} = \frac{I}{eV} - \frac{N}{\tau_e} - \sum_m \upsilon_g g(\lambda_m)S_m \tag{11a}$$

$$0 = \frac{dS_m}{dt} = \upsilon_g \Gamma g(\lambda_m) S_m + B\beta N^2 - \frac{S_m}{\tau_l} \tag{11b}$$

where I is the injection current, V is the volume of active layer, β is the spontaneous emission factor, υ_g is the group velocity, Γ is the confinement factor, τ_e is the carrier lifetime and is given by

$$\tau_e = \frac{1}{A + BN + CN^2} \tag{12}$$

where A is the nonradiative recombination rate, B is the radiative recombination coefficient, C is the auger recombination coefficient. $g(\lambda_m)$ is the gain of mth mode and is given by:

$$g(\lambda_m) = g_0[1 - (\frac{\lambda_m - \lambda_g}{\Delta\lambda_g})^2] \tag{13}$$

where $g_0 = a(N - N_0)$, a is the gain constant, λ_g is the center wavelength of the gain, $\Delta\lambda_g$ is the 3dB bandwidth of the gain. τ_l is the photon life of each mode and is given by $1/\tau_l = 1/\tau^{cav} + 1/\tau^{scatt}$, where τ^{scatt} is the lifetime due to scatter loss, which is the same for each mode; τ_l^{cav} is the external cavity lifetime, for our system, τ_l^{cav} is a variable and calculated from the expression:

$$\tau_l^{cav} = \frac{\int_{z_0}^{z_1}\langle U_1(z)\rangle dz + \int_{z_1}^{z_2}\langle U_2(z)\rangle dz + \int_{z_2}^{z_3}\langle U_3(z)\rangle dz + \int_{z_3}^{z_4}\langle U_4(z)\rangle dz}{2\sqrt{\frac{\varepsilon_0}{\mu_0}}(\eta_0|A_0|^2 + \eta_5|B_5|^2)} \tag{14}$$

where the cycle-averaged energy densities $\langle U_1(z)\rangle$, $\langle U_2(z)\rangle$, $\langle U_3(z)\rangle$ and $\langle U_4(z)\rangle$ are given by

$$\langle U_1(z)\rangle = 2\varepsilon_0\eta_1^2(|A_1|^2 e^{-g_{th}z} + |B_1|^2 e^{g_{th}z}) \tag{15a}$$

$$\langle U_2(z)\rangle = 2\varepsilon_0\eta_2^2(|A_2|^2 + |B_2|^2) \tag{15b}$$

$$\langle U_3(z)\rangle = 2\varepsilon_0\eta_3^2(|A_3|^2 + |B_3|^2) \tag{15c}$$

$$\langle U_4(z)\rangle = 2\varepsilon_0 n_{eff}^2(\frac{|A_4|^2 + |A_5|^2 + |B_4|^2 + |B_5|^2}{2}) \tag{15d}$$

On evaluating the integrals, the external cavity lifetime is given by:

$$\tau_l^{cav} = \frac{\frac{\eta_1^2}{g_{th}}[|A_1|^2(e^{-g_{th}z_0} - e^{-g_{th}z_1}) + |B_1|^2(e^{g_{th}z_1} - e^{g_{th}z_0})] + (|A_2|^2 + |B_2|^2)(z_2 - z_1)\eta_2^2 + (|A_3|^2 + |B_3|^2)(z_3 - z_2)\eta_3^2 + (\frac{|A_4|^2 + |B_4|^2 + |B_5|^2}{2})Lg\,n_{eff}^2}{c\cdot(\eta_0|A_0|^2 + \eta_5|B_5|^2)} \tag{16}$$

Based on the above analysis, for a FGL of given parameters, the S_m can be specified and the output power of the mth mode can be calculated by:

$$P_m = \frac{(1-R_1)|r_0|}{(1-R_1)|r_0| + (1-R_1)|r_1|}\frac{hc}{\lambda_m}\upsilon_g(-\frac{1}{L_d}\ln|r_0 r_1|)VS_m \tag{17}$$

where h is the plank constant, $r_0 = B_1/A_1$ is the reflection coefficient of LD rear facet, $r_1 = [A_1\exp(-ik_1L_d)]/[B_1\exp(ik_1L_d)]$ is the reflection coefficient of LD front facet.

From (17), the SMSR of the FGL can be obtained and defined as:

$$SMSR = 10\lg(\frac{P_0}{P_1}) \tag{18}$$

where P_0 is peak power within the FG reflection bandwidth, P_1 is the peak power outside the reflection bandwidth.

3. Results and discussion

The data used in calculations are: L_d = 250μm, L_a = 8.1 μm, L_e = 1×10^{-3} m, V = 1×10^{-16}m^3, e = 1.6×10^{-19}C, β = 1×10^{-4}, Γ = 0.3, h = 6.63×10^{-34}Js, α = 2.5×10^{-20}m^2, υ_g = 0.75×10^8 m/s, τ^{scatt} = 1.7ps, N_0 = 1×10^{-24}m^{-3}, λ_g = 1550.1 nm, $\Delta\lambda_g$ = 10nm, λ_B = 1548.8 nm, A = 1×10^8s^{-1}, B = 1×10^{-16}m^3/s, C = 3×10^{-41}m^6/s, η_0 = 1, η_{a1} = 3.5, b = 1×10^{-26}m^3, η_2 = 1, η_3 = 1.45 , n_{eff} = 1.46 , η_5 = 1.45, G = 10, L_g = 2 mm.

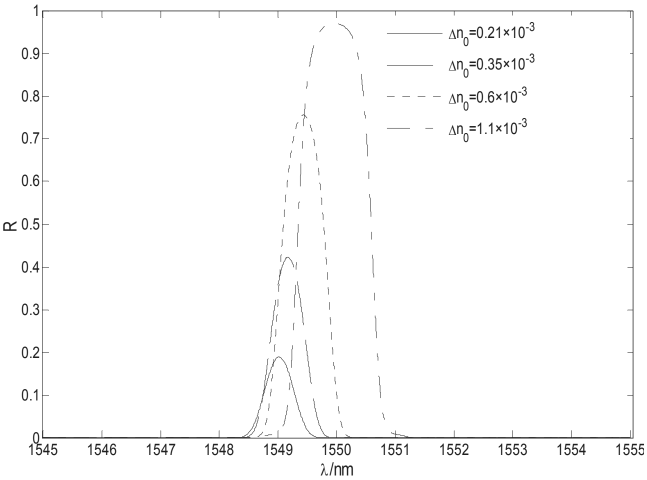

Fig.2. Reflection spectrum of the Gaussian apodized FG for different Δn_0.

Fig. 2 gives the reflection spectrum of the Gaussian apodized FG for different Δn_0. Compared with the uniform FG, the sidelobes have been suppressed efficiently. With the increase of Δn_0, the peak reflectivity increases, the wavelength corresponding to peak reflectivity shifts to long wavelength and the full-width-half-maximum (FWHM) increases. Here we consider the weak feedback case, which means no antireflection coating at the front facet of the LD. It is assumed that the light outputs from the FG. Fig. 3 shows the output spectrum of the FGL for different Δn_0. From this diagram, it can be seen that the FGL is the single-mode output, the modes outside 3dB bandwidth of FG have been suppressed efficiently and the lasing wavelength appears within 3dB bandwidth of FG and shifts towards long wavelength with the increase of Δn_0. Moreover, the single mode operation with the side-mode suppression ratio (SMSR) more than 40dB can be obtained. These can be explained as that with the change of the maximum of the refractive index modulation depth Δn_0, the peak reflectivity, 3dB bandwidth and the center wavelength of FG will vary as Fig.2. Owing to the contribution of the FG, the mode distribution of FGL will vary, the most intense side mode may no longer be the mode nearest to the peak mode, and the wavelength interval between the peak mode and the most intense side mode maybe change (increase or decrease) with the change of Δn_0. So the mode competition will induce the change of the number, the location and the power of the modes.

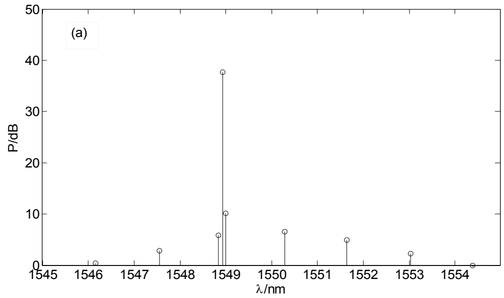

(a)

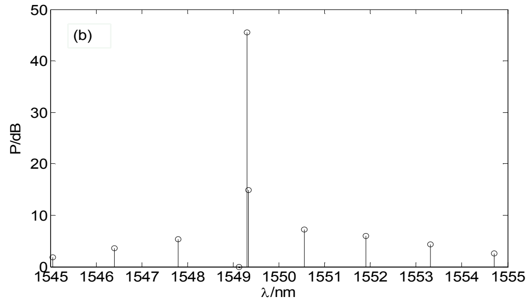

(b)

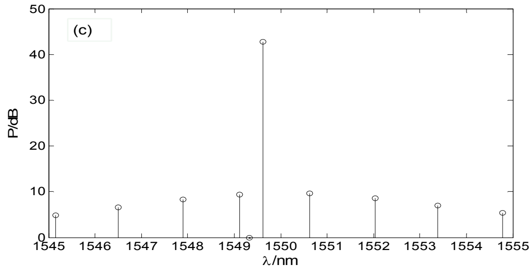

(c)

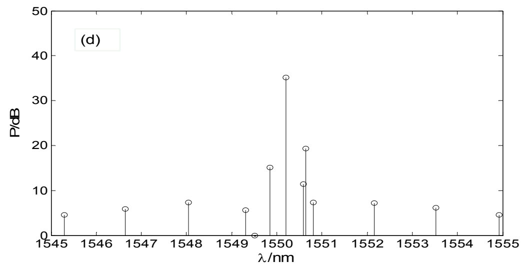

(d)

Fig.3. Output spectrum of the apodized FGL with (a) $\Delta n_0=0.21\times10^{-3}$, (b) $\Delta n_0=0.35\times10^{-3}$, (c) $\Delta n_0=0.6\times10^{-3}$, (d) $\Delta n_0=1.1\times10^{-3}$.

Fig. 4 gives the corresponding P-I curves for these Δn_0. From this diagram, it can be observed that the threshold current is about 16mA for different Δn_0. With the increase of the Δn_0, the output power tends to decrease on the whole. When Δn_0 =0.35×10^{-3}, it has a largest output power and the slope is about 0.28 mW/mA. When Δn_0 = 1.1×10^{-3} and Δn_0 = 0.6×10^{-3}, the output power become smaller and the slope is about 0.07 mW/mA and 0.015 mW/mA, respectively.

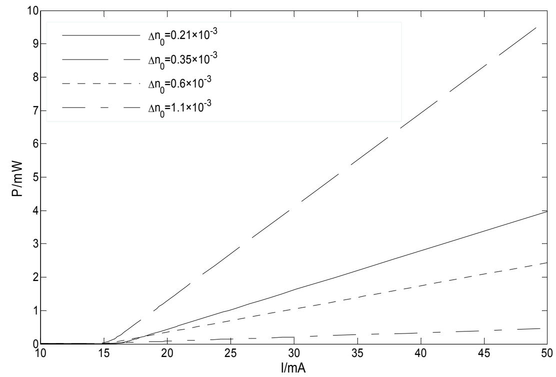

Fig. 4. P-I curve for different Δn_0.

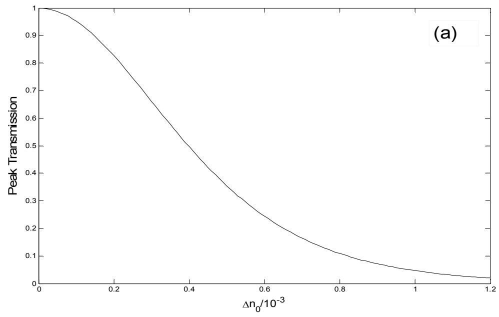

(a)

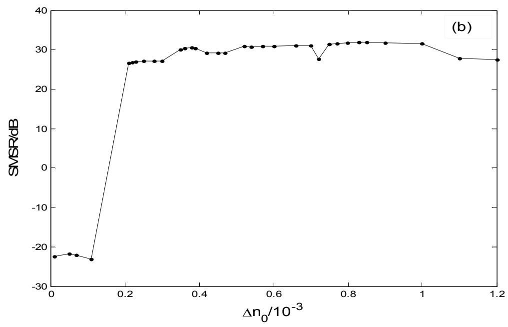

(b)

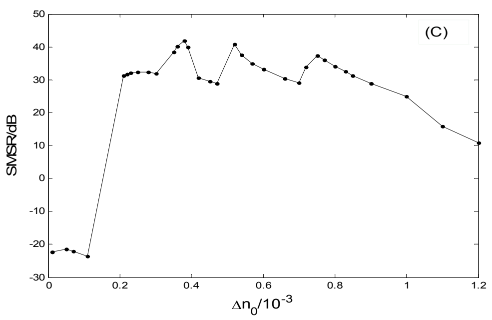

(c)

Fig. 5. (a) Peak transmission of the apodized FG vs. Δn_0. (b) SMSR of the optical spectrum in the internal cavity vs. Δn_0 (I=40mA). (c) SMSR of the output spectrum of FGL vs. Δn_0 (I=40mA).

This can be interpreted as that with the increase of Δn_0 the peak transmission decreases obviously as shown in Fig. 5(a). So the output power will become smaller. However, when $\Delta n_0=0.21\times10^{-3}$, the slope is $0.11\, mW / mA$. The result does not accord with above varying tendency. This can be interpreted as that with the increase of Δn_0, on the one hand, the peak reflectivity of FG becomes larger, which is helpful to suppression of the main mode to the side mode. On the other hand, with the increase of the peak reflectivity the output power will decrease. So an optimal Δn_0 should be selected for better output.

Fig. 5(a) shows the variation of peak transmission of the apodized FG with Δn_0. From this diagram, it can be observed that with the increase of Δn_0, the peak transmission intensity will decrease.

Fig. 5 (b) shows the variation of SMSR of the optical spectrum in internal cavity with Δn_0 for I=40mA. Fig. 5 (c) shows the variation of the SMSR of the output spectrum of FGL with Δn_0 for I=40mA.

From these diagrams, it can be seen that when Δn_0 is small, a negative SMSR appears. With the increase of Δn_0, SMSR become positive. Moreover, the SMSR of output spectrum of FGL undergoes a significant fluctuation. These phenomena can be explained as that when Δn_0 is small, FGL oscillates at a wavelength outside the FG 3dB bandwidth. So the SMSR is negative. With the increase of Δn_0, on the one hand, peak reflectivity of FG will increase, which is helpful to suppression of the main mode to the side mode. On the other hand, as mentioned above, the mode distribution of FGL will vary. After taking into account the contribution of FG and the wavelength dependence of the gain profile of the LD medium, an oscillation of the SMSR with Δn_0 can be comprehended.

4. Conclusions

By using transfer matrix method, after considering the gain distribution with wavelength, the wavelength of each output mode has been obtained. Combining with the multimode rate equations, the effect of the maximum refractive index modulation depth Δn_0 of the Gaussian apodized FG on the output characteristics of FGLs have been investigated. With the change of the maximum of the refractive index modulation depth Δn_0, both the number and the location of the modes will undergo variations. The modes outside the 3dB bandwidth of FG have been suppressed efficiently and single mode operation with the side-mode suppression ratio (SMSR) more than 40dB can be achieved. We hope this work will be helpful to provide a profound insight to the FGLs.

Acknowledgements

This work was supported by the Natural Science

Foundation Project of Chongqing City (CQ CSTC) of China, and the High-Tech Nurtured Fund of the Southwest University of China.

References

[1] W. H. Cheng, S. F. Chiu, C. Y. Hong, H. W. Chang, "Spectral characteristics for a fiber grating external cavity laser," Opt. & Quantum Electron. **32**, 339 (2000).
[2] T. Deng, G. Xia, Z. Wu, "Influence of the optical feedback on the large signal modulation characteristics of the external cavity semiconductor laser," J. Mater. Sci.: Mater. Electron. **17**, 301 (2006).
[3] Z. Wu, G. Xia, J. Wu, "Studying the extremely short external cavity semiconductor laser with ray tracing method," Opt. Commun. **279**, 336 (2007).
[4] G.. Xia, Z. Wu, H. Zhou, "Influence of external cavity length on lasing wavelength variation of fiber grating semiconductor laser with ambient temperature," Optik **114**, 247 (2003).
[5] R. Lang, K. Kobayashi, "External optical feedback effects on semiconductor injection laser properties," IEEE J. Quantum Electron. **16**, 347 (1980).
[6] A. T. Ryan, G. P. Agrawal, G. R. Gray, E. C. Gage, "Optical-feedback-induced chaos and its control in multimode semiconductor lasers," IEEE, J. Quantum Electron. **30**, 668 (1994).
[7] H. Kakiuchida, J. Ohtsubo, "Characteristics of a semiconductor laser with external feedback," IEEE J. Quantum Electron. **30**, 2087 (1994).
[8] I. Pierce, P. Rees, P. S. Spencer, "Multimode dynamics in laser diodes with optical feedback," Phys. Rev. A **61**, 053801 (2000).
[9] D. Pastor, J. Capmany, D. Ortega, V. Tatay, J. Marti, "Design of apodized linearly chirped fiber gratings for dispersion compensation," J. Lightwave Technol. **14**, 2581 (1996).
[10] C. Martinez, S. Magne, P. Ferdinand, "Apodized fiber Bragg gratings manufactured with the phase plate process," Appl. Opt. **41**, 1733 (2002).
[11] T. Erdogan, "Fiber grating spectra," J. Lightwave Technol.**15**, 1277 (1997).
[12] M. Yamada, K. Sakuda, "Analysis of almost periodic distributed feedback slab waveguides via a fundamental matrix approach," Appl. Opt. **26**, 3474 (1987).
[13] G. Xia, Z. Wu, J. Chen, Y. Lu, "Studying semiconductor lasers with multimode rate equations," Appl. Opt. **34**, 1523 (1995).

*Corresponding author: gqxia@swu.edu.cn